6-2018

Analysing multi-point multi-frequency machine vibrations using optical sampling

Dibyendu ROY

Avik GHOSE

Tapas CHAKRAVARTY

Sushovan MUKHERJEE

Arpan PAL

See next page for additional authors

Analysing Multi-Point Multi-Frequency Machine Vibrations using Optical Sampling

Dibyendu Roy
TCS Research and Innovation
Kolkata, India
roy.dibyendu@tcs.com

Avik Ghose
TCS Research and Innovation
Kolkata, India
avik.ghose@tcs.com

Tapas Chakravarty
TCS Research and Innovation
Kolkata, India
tapas.chakravarty@tcs.com

Sushovan Mukherjee
TCS Research and Innovation
Kolkata, India
sushovan.mukherjee@tcs.com

Arpan Pal
TCS Research and Innovation
Kolkata, India
arpan.pal@tcs.com

Archan Misra
Singapore Management University
Singapore
archanm@smu.edu.sg

ABSTRACT

Vibration analysis is a key troubleshooting methodology for assessing the health of factory machinery. We propose an unobtrusive framework for at-a-distance visual estimation of such (possibly high frequency) vibrations, using a low fps (frames-per-second) camera that may, for example, be mounted on a worker's smartglass. Our key innovation is to use an external stroboscopic light source (that, for example, may be provided by an assistive robot), to illuminate the machine with multiple mutually-prime strobing frequencies, and use the resulting aliased signals to efficiently estimate the different vibration frequencies via an enhanced version of the Chinese Remainder Theorem. Experimental results show that our technique estimates multiple such frequencies faster, and compares favourably to an equipment-mounted accelerometer alternative, with frequency estimation errors below 0.5% for vibrations occurring up to 500 Hz.

CCS CONCEPTS

• **Computer systems organization** → **Embedded systems**; *Redundancy*; Robotics; • **Networks** → Network reliability;

KEYWORDS

Unobtrusive Multi-frequency Vibration Measurement, Optical Sampling, Frequency Estimation, Chinese Remainder Theorem

ACM Reference Format:

Dibyendu Roy, Avik Ghose, Tapas Chakravarty, Sushovan Mukherjee, Arpan Pal, and Archan Misra. 2018. Analysing Multi-Point Multi-Frequency Machine Vibrations using Optical Sampling. In *Proceedings of June 10, 2018, Munich, Germany (IoPARTS'18,June 10, 2018, Munich, Germany)*. ACM, New York, NY, USA, 5 pages. https://doi.org/10.1145/3215525.3215529

IoPARTS'18,June 10, 2018, Munich, Germany, 2018

ACM ISBN 978-1-4503-5843-9/18/06...$15.00
https://doi.org/10.1145/3215525.3215529

1 INTRODUCTION

Machine condition monitoring [7] is a critical part of industry operations, with such monitoring being used to both continuously optimize the machine's operating parameters and to detect anomalous behaviour that can culminate in breakdowns. Vibration, acoustic and temperature data are commonly used as external indicators of the internal state of such machines. Analysis of vibration data, typically collected from machine-mounted accelerometers, is widely used as a first indicator of potential machine faults. More specifically, for machines with rotating components, spectral analysis of vibration signals can provide important insights on their working and mechanical conditions, such as the accuracy of shaft alignment and balance, the condition of bearings or gears, or resonance effects generated from the housings, piping or other structures. As assistive robots increasingly become part of manufacturing environments, it is useful to investigate their possible use, in tandem with personal wearable sensors, for novel forms of machine diagnostics.

Existing Practice and Limitations: Machine vibration is commonly measured using accelerometers or velocity sensors. However, such sensors need to be mounted on the equipment being monitored, and thus poses deployment and operating challenges in hazardous environments e.g., when being operated under high temperature or pressure conditions. Non-contact approaches for vibration measurement are thus attractive alternatives. Two such non-contact strategies include Laser Doppler Vibrometry (LDV) [1] and Near-field Acoustic Holography (NAH) [4]. These techniques either require a set of carefully synchronized lasers or utilize pressure readings on a surface that is very close to (but not attached to) the vibrating surface. LDV can offer very accurate vibration frequency estimates, but requires expensive equipment and it is very slow to inspect the vibration of a large surface. Camera-based vibration estimation [2], which relies on the processing of a series of image frames captured by a video sensor, offers a compelling at-a-distance alternative to these techniques. Measuring high-frequency vibrations accurately, however, requires the use of specialized, expensive, very high frame rate (e.g., 1000 fps) cameras [5], to avoid the 'aliasing' problem. In our recent work [8], [9], we have proposed an alternative approach, called the *ShakeMeter*, for measuring such high frequency vibration using a commodity low-speed (30fps) camera. The key idea is to utilize a high frequency optical stroboscope [11] that effectively modulates the vibration signal, shifting the frequency components within the camera's Nyquist frequency. However, such prior work is based on a single strobing rate and can measure only a single (or at most two) distinct frequency.

Contribution: In this work, we consider the problem of using a low-fps camera to optically estimate the vibration of a rotating machine, when the vibration consists of multiple distinct frequencies. Note that the number of such frequencies is not known a-priori, and may not be harmonics of one another. We make the following contributions:

- *Propose a multi-frequency strobing strategy:* To infer multiple unknown vibration frequencies, we propose an approach where the stroboscope is operated sequentially at multiple mutually-prime frequencies. (Our proposed approach may be implemented using human-robot collaboration, where the robot acts as the strobing source, in tandem with a wearable camera worn by a worker.) We develop the mathematical framework that expresses the aliasing effect created by the use of such mutually-prime strobe frequencies.
- *Efficient frequency estimation algorithm:* We develop and demonstrate an algorithm for multi-frequency vibration estimation, based on a novel application of the Chinese Remainder Theorem (CRT). Our approach is much faster than the alternative approach of incrementally increasing the strobing frequency. It works on the residual set of p frequencies obtained by each of the distinct strobing frequencies, estimating the lowest unknown frequency component first, before iteratively re-applying it on the remaining $p-1$ set of unknown frequencies.
- *Experimental validation:* We experimentally demonstrate that our purely at-a-distance low-fps approach can indeed estimate multiple frequencies, with an estimation error (0.12%) that is equivalent to that obtained (0.08%) by a physically-mounted accelerometer.

More broadly, this work introduces the possibility of *jointly* using IoT devices (e.g., programmable LED bulbs or light probes from a robot) and personal wearable devices (e.g., smartglass-mounted cameras) to provide fine-grained monitoring of factory operations.

2 STROBOSCOPIC PRINCIPLE

We first mathematically express the impact of strobing and low-fps video capture on the vibration signal. Assuming an unknown periodic vibrating signal $w(t)$ is sampled by a strobe–i.e., an infinite optical pulse train (*Dirac comb*) $p(t) = \sum_{n=-\infty}^{\infty} \delta(t - nT_s)$ of known period T_s. Then the resulting sampled signal $w_s(t)$ can be expressed as;

$$w_s(t) = w(t) \times p(t) \tag{1}$$

$$W_s(\omega) = \frac{1}{2\pi}[W(\omega) \circledast P(\omega)] \tag{2}$$

where $W_s(\omega)$ and $P(\omega)$ are the fourier spectrum of $w_s(t)$ and $p(t)$. Then $P(\omega)$ can be written as;

$$P(\omega) = \frac{2\pi}{T_s} \sum_{k=-\infty}^{\infty} \delta(\omega - k\omega_s) \tag{3}$$

where $k \in \mathbb{Z}^+$ and ω_s is the frequency of the optical sampling. Then $W_s(\omega)$ will be;

$$W_s(\omega) = \frac{1}{T_s} \sum_{k=-\infty}^{\infty} W(\omega - k\omega_s) \tag{4}$$

This sampled signal is then captured by a low fps camera, having frame rate of ω_{cam}. The camera effectively acts as a low pass filter (LPF) of cut-off frequency of ω_{cam}. The system needs to maintain the following principles.

2.1 Condition of Strobing

From Equation 4, it is well understood that aliased frequencies will be observed, unless the camera sampling rate is grater than or equal to twice of $(\omega - k \times \omega_s)$ (Nyquist sampling criteria [3]). Therefore, the condition of aliasing-free strobing can be written as;

$$2 \times |\omega - k \times \omega_s| \leq \omega_{cam} \tag{5}$$

Moreover, aliased frequency can also be observed because of frequency folding phenomena, which can be written as;

$$2 \times ||\omega - k \times \omega_s| - \omega_{cam}| \leq \omega_{cam} \tag{6}$$

We thus see that the aliased frequency will fall within the camera's sampling frequency, only if the above condition is satisfied. More specifically, if k can be estimated, then the unknown vibration frequency ω can be obtained properly.

3 SYSTEM DESIGN AND IMPROVEMENT ON IMAGE PROCESSING

We now briefly describe our set up to study the joint impact of strobing and low-fps image capture. In our current work, we have recreated a laboratory version of our envisioned infrastructure: this laboratory version consists of a frequency-tunable audio speaker (representing the machine being analyzed) and a programmable LED array. As shown in Fig. 1, our system contains an array (20×20) of LED panel (for optical sampling), along with a 30-fps optical camera. To get sub-multiple effects from the optical sampler, the LEDs should be 'ON' for a very short duration [11]. So, in our experiment we have chosen 1% duty cycle for the optical sampler. Initially, a 60 Hz pulse train with 1% duty cycle is produced in optical sampler and used to illuminate the rotating machine. The resultant images are captured by the camera. For easy tracking of the resulting rotational movement, a specific visual marker is attached to the machine (details of the procedure can be found in [8] and the entire system's performance analysis on different environmental conditions can be founed in [6]), and the frequency spectrum is computed from the time series representing the marker's displacement pattern. Based on the signal-to-noise ratio (SNR) of the resultant frequency spectrum, the frequency of the pulse train (in optical sampler) is increased.

Marker Enhancement: In [8], [9], the tracking was performed on white image. However, white image can be split into red, green and blue channel as shown in Fig. 2.(a). When we separately tracked each of the RGB channels, we observed (see Fig. 2(b)) that the SNR obtained was highest for the green image. Accordingly, for improved accuracy, we only track the green channel of the marker.

In our previous work [8], we applied an incremental approach of ω_s, to estimate the value of k as well as ω. We utilize this same *Incremental* strategy as our baseline for the problem of multiple frequency vibration detection. However, we shall see that the esti-

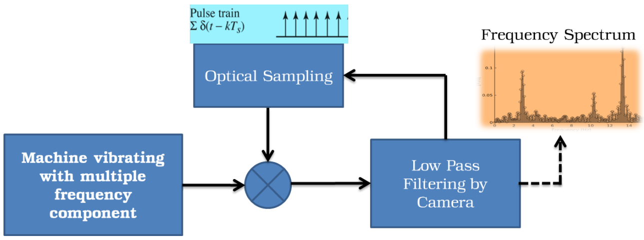

Figure 1: System Framework.

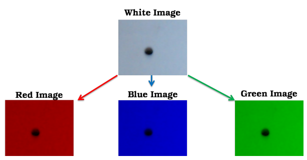

(a) Image Split for SNR Improvement

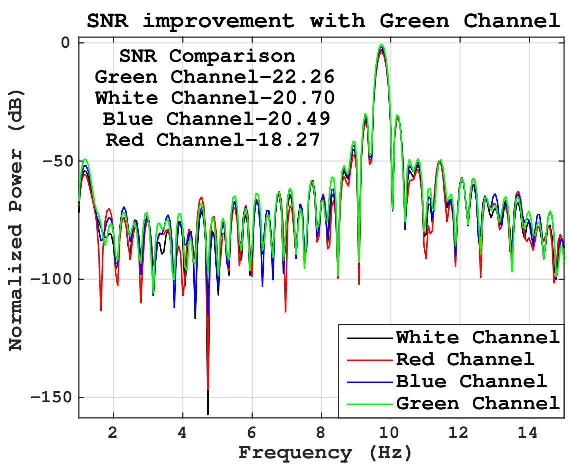

(b) Signal-to-Noise Ratio Plot

Figure 2: SNR Improvement on Green Image Tracking.

mation process takes significantly longer, especially when multiple frequencies are present.

4 MULTIPLE FREQUENCY VIBRATION DETECTION

We now extend our analysis to the case where the vibrating signal $w(t)$ having multiple frequency components $[w_1(t), w_2(t), ..., w_N(t)]$. As before, it is sampled by a probe $p(t)$ having sampling frequency ω_s. Then the resultant signal $w_s(t)$ will be;

$$w_s(t) = \sum_{i=1}^{N}[w_i(t) \times p(t)] \tag{7}$$

In frequency domain, the above equation can be written as;

$$W_s(\omega) = \frac{1}{T_s}\sum_{k=1}^{\infty}[\sum_{i=1}^{N} W_i(\omega_i - k\omega_s)] \tag{8}$$

Therefore, for multiple frequency vibration detection, the condition of strobing can be written as (section 2.1);

$$\begin{gathered}\sum_{i=1}^{N}|\omega_i - k \times \omega_s| = \omega_{observed} \\ \sum_{i=1}^{N}||\omega_i - k \times \omega_s| - \omega_{cam}| = \omega_{observed}\end{gathered} \tag{9}$$

where $\omega_{observed}$ is the observed frequency by the camera. In order to get some meaningful insight about the aliased frequency components, ω_{cam} should be always greater than or equal to twice of $\omega_{observed}$, i.e., $\omega_{observed} \leq |\omega_{cam}/2|$.

4.1 Necessary and Sufficient Condition

Assume that $w(t)$ is optically sampled by $\omega_s = [\omega_{s_1}, \omega_{s_2}, ..., \omega_{s_p}]$. Then frequency determination is only possible if and only if $max[\omega_{s_i}] \geq max[\omega_j]$, where $i \in [1, 2, ..., p]$ and $j \in [1, 2, ..., N]$. In other words, the optical sampler should have some prior knowledge about $max[\omega_j]$– i.e., it needs an upper bound on the highest feasible vibration frequency. Otherwise, detected frequencies have modulo ambiguities [12].

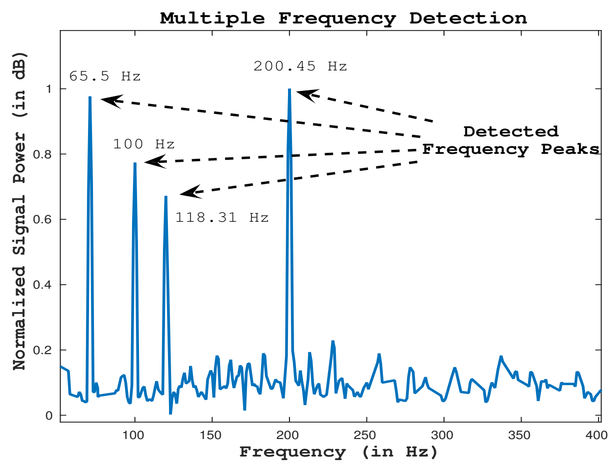

Figure 3: Multiple Frequency Detection.

For each sampling instances $\omega_{s_i}; i \in [1, 2, ..., p]$, a set of $\omega_{observed}$ is obtained; if $SNR[\omega_{observed}]$ is above some acceptable limit. Therefore, for each r; $1 \leq r \leq p$, the residue set $S_r(\omega_1, \omega_2, ..., \omega_N)$ can be estimated from 9, assuming $k \in \mathbb{Z}^+$ and $\omega_{cam} = 30$. The final residue set S will be $S = [S_1, S_2, ..., S_r]$. Then the multiple frequency estimation function [10] can be written as;

$$\hat{f}_h(S) = \frac{1}{nh}\sum_{i=1}^{n} K(\frac{S - S_i}{h}) \tag{10}$$

where K is the kernel (non-negative function) and $h > 0$ is the smoothing parameter and n is the no of element is S. Fig. 3 represents the multiple frequency detection plot of the above stated approach.

Limitation: In our baseline *Incremental* approach, ω_{s_i} is increased by '1' Hz in each iteration until $\omega_{s_{i+1}} > max[\omega_j]$. This proces can have very high latency [13]. To reduce this estimation latency, we need to both (i) develop a non-incremental approach to choosing the set ω_s, and (ii) estimate ω_j, such that $max[\omega_{s_i}] < max[\omega_j]$. So, the main challenge for us is to efficiently remove the "modulo ambiguities".

5 DETECTION IMPROVEMENT USING CHINESE REMAINDER THEOREM BASED APPROACH

To overcome the modulo ambiguities, a novel application of the Chinese Remainder Theorem (*CRT*) [15], [14] is applied on S, presuming $k \in \mathbb{Z}^+$ and $\omega_{cam} = 30$. However, for the successful convergence, the sampling set $\omega_s = [\omega_{s_1}, \omega_{s_2}, ..., \omega_{s_p}]$ should be co-prime in nature, which is the main condition of CRT. Now the problem reduces to determining $[\omega_1, \omega_2, ..., \omega_N]$ from the residue set S. The likely presences of multiple frequencies, however, makes the more complex because the residue set does not specify the order of the residues $\omega_{observed_{j,r}}$ with respect to j but only r sets of numbers. Consequently, we adopt an iterative approach, whereby the multiple frequency can be estimated iteratively on the residue set of p frequencies obtained by each $\omega_{s_i}; i \in p$, estimating the smallest unknown frequency first, before re-applying the approach on the remaining $p-1$ set of unknown frequencies.

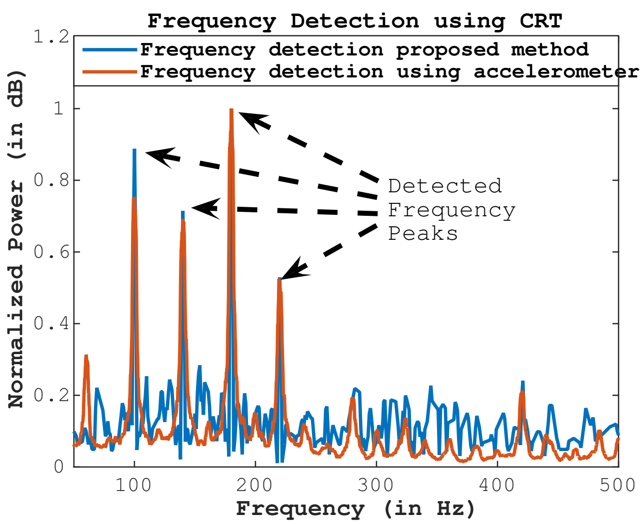

Figure 4: Multiple Frequency Detection using CRT.

Detection Algorithm: The detail steps for the multiple frequency vibration detection are given below;

Step 1: Take an arbitrary vector set $(k_1, k_2, ..., k_p) \in S$.

Step 2: For each $1 \le r \le p$, define a set;

$$\Gamma_r = \{k_r + n \times \omega_{s_r}; k_r \le k_r + n \times \omega_{s_r}\}$$

where n is an integer. All numbers in Γ_r have same residue modulo ω_{s_r}, which is called as coset of k_r.

Step 3: There exist integers $r_1, r_2, .., r_\alpha$ with $1 \le r_1 < r_2 < ... < r_\alpha \le p$, such that the residues $k_{r_1}, k_{r_2}, ..., k_{r_\alpha}$ are from a common frequency (i.e., $\tau = \Gamma_{r_1} \cap \Gamma_{r_2} \cap ... \cap \Gamma_{r_\alpha} \neq \emptyset$). So $\tau = \{\bar{N}\}$.

Now check whether $\bar{N}$ is a valid frequency by checking if its residue vector $(\bar{k_1}, ..., \bar{k_p}) mod(\omega s_1, ..., \omega s_p)$ belongs to the set S. If not, find another set of $1 \le r_1 < r_2 < ... < r_\alpha \le p$, such that $\tau = \Gamma_{r_1} \cap \Gamma_{r_2} \cap ... \cap \Gamma_{r_\alpha} \neq \emptyset$. Repeat the step, until N is a valid frequency denoted by $N_N \in \Gamma$.

Step 4: For $r = 1, 2, ..., p$, remove $k_{p,r} = N_N mod \omega_{s_r}$ from S_r.

Step 5: Go to step 1 by replacing p with $p-1$ and replace $S(N_1, N_2, ..., N_p)$ with $S(N_1, N_2, ..., N_{p-1})$. Repeat the step until all N are determined.

6 PERFORMANCE RESULTS

We first experimentally study the accuracy of our proposed algorithm, compared to an accelerometer-based [5] alternative. Multi-frequencies (100, 140, 180 & 220 Hz) are generated in an audio speaker (Fig. 5) with a mobile phone. The raw accelerometer data is processed by a 10-point moving average filter. Fig. 4 shows the comparative estimation between our proposed CRT-based visual method and the accelerometer-based approach. Accelerometer-based sensing results in a *mean frequency estimation error* of 0.08%, compared to 0.12% for our proposed approach (the entire results are shown in Table 1).

Table 1: Error Comparison (upto 500 Hz)

No. of Frequencies	Accelerometer	Proposed Method
3	0.07%	0.09%
4	0.08%	0.12%

The results demonstrate that our at-a-distance visual monitoring technique can provide an effective and unobtrusive alternative.

Next, we compare the convergence time of our proposed technique to the baseline (incremental) approach. The results are provided in Table 2. We observe that the incremental technique takes significantly longer to detect independent vibrational frequencies, with the duration increasing *super-linearly* with the number of frequencies. In particular, when the vibrating system has 7 component frequencies, the incremental approach fails to converge within an experimental bound of 1500 secs. In contrast, our proposed method, based on mutually-prime strobe frequencies estimates frequencies within our stipulated time, finishing, in all cases, within 350 secs. While the approximately 6 minute duration can appear to be high, we shall later discuss that the estimation procedure need not be *continuous*, but can in fact stitch together observations from multiple non-contiguous time windows.

Table 2: Performance Comparison (upto 500 Hz)

No. of Frequencies	Baseline (sec.)	Proposed (sec.)
2	100-450	75-180
4	100-1500	75-220
7	>1500	75-350

6.1 Multi-Point Vibration Detection:

We also study the use of our visual technique for cases where different parts of the machine vibrate at different frequencies. For such situations, an accelerometer-based approach may not be ideal, as it would require placing a separate accelerometer at each location–i.e., we will need prior knowledge about the movement behavior of the machine. In contrast, an optical camera-based approach can *independently monitor the vibration frequency of different visual markers*-i.e., different locations on the same machine. As an example, Fig. 5 shows an experimental setup, where two different parts vibrate at different (and possibly multiple frequencies). Our CRT-based visual approach is able to track both vibrations separately, achieving a mean detection error rate of 0.44% for Point 1 and 0.18% for Point 2. Our results suggest that our low-fps camera-based approach can be more powerful than traditional sensing systems in this regards.

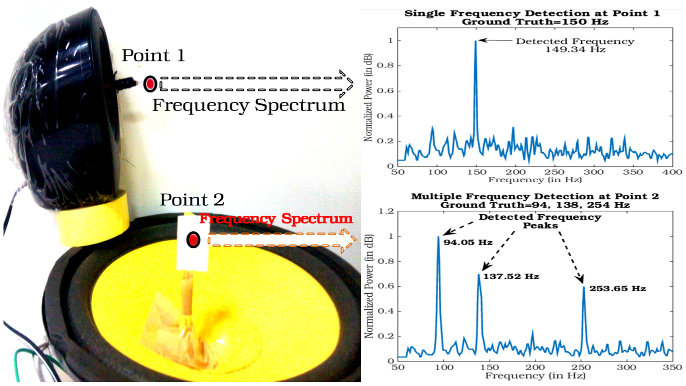

Figure 5: Multiple Point Frequency Detection.

7 DISCUSSION

We believe that our work illustrates the promise of such optical sampling-based frequency estimation. However, there are several additional issues to consider and challenges to solve before we can realize a complete practical system.

Moving to Wearable Sensing: At present, our system utilized a fixed, low-fps camera. Our vision is to replace this with a smartglass-mounted camera, that unobtrusively captures such image samples as a factory worker goes about his regular work. In this case, the smartglass's field of view will change continually, and we will need additional fusion of wearable inertial sensor data to first estimate the field-of-view of the wearable camera, prior to our frequency analysis. Moreover, the overall system design will then also need to consider the energy overheads of such continuous image capture. As a consequence, it is likely that the optical sampling process (for a particular machine) will not be continuous, but obtained in a bursty fashion (a set of temporally separated segments). We will have to adapt our estimation algorithms to account for such non-contiguous observations.

Use of Smart LEDs or Assistive Robots: Our current system utilizes a single LED panel, with strobing performed sequentially. Our eventual vision is to embed such high-frequency strobing as part of smart lighting equipment–i.e., using the spatially distributed set of LED bulbs on the factory floor. In this case, each bulb might have an independent strobing mechanism, and the resulting illumination at any one location will be due to the superposition of multiple *concurrent* spatially distributed strobes. Alternatively, the light source may come from a collocated robot, such that it updates its directional light beam continually based on real-time information on the worker's *visual pose*–i.e., the direction of the field-of-view of the worker's smartglass. These approaches will require us to modify and enhance our estimation process.

8 CONCLUSION

We proposed an unobtrusive, optical sensing approach that uses cleverly selected strobing frequencies to detect an equipment's vibration frequencies. We show that our system is capable of detecting multiple frequencies efficiently, with estimation errors below 0.1% and convergence times that are 3-8 times lower than a baseline incremental method. Our system can also be applied to situations where different machine parts exhibit distinct vibration behavior. In ongoing work, we shall explore the development of an integrated framework, where such strobing is combined with wearable-mounted cameras to provide continuous sensing of factory equipments in an opportunistic fashion.

REFERENCES

[1] P Castellini, M Martarelli, and EP Tomasini. 2006. Laser Doppler Vibrometry: Development of advanced solutions answering to technology's needs. *Mechanical Systems and Signal Processing* 20, 6 (2006), 1265–1285.

[2] Justin Gejune Chen. 2016. *Video camera-based vibration measurement of infrastructure.* Ph.D. Dissertation. Massachusetts Institute of Technology.

[3] Luc Lévesque. 2014. Nyquist sampling theorem: understanding the illusion of a spinning wheel captured with a video camera. *Physics Education* 49, 6 (2014), 697.

[4] M Martarelli and GM Revel. 2006. Laser Doppler vibrometry and near-field acoustic holography: Different approaches for surface velocity distribution measurements. *Mechanical systems and signal processing* 20, 6 (2006), 1312–1321.

[5] PD McFadden and JD Smith. 1984. Vibration monitoring of rolling element bearings by the high-frequency resonance techniqueâĂŤa review. *Tribology international* 17, 1 (1984), 3–10.

[6] Prasant Misra, Dibyendu Roy, Tapas Chakravarty, and Arpan Pal. 2017. Unobtrusive vibration sensing using optical strobing: Performance analysis. In *Sensing Technology (ICST), 2017 Eleventh International Conference on.* IEEE, 1–4.

[7] Amiya Ranjan Mohanty. 2014. *Machinery condition monitoring: Principles and practices.* CRC Press.

[8] Dibyendu Roy, Sushovan Mukherjee, Brojeshwar Bhowmik, Arijit Sinharay, Ranjan Dasgupta, and Arpan Pal. 2016. An autonomous, non-invesive vibration measurement system using stroboscope. In *Sensing Technology (ICST), 2016 10th International Conference on.* IEEE, 1–6.

[9] Dibyendu Roy, Sushovan Mukherjee, Tapas Chakravarty, Arijit Sinharay, Avik Ghose, and Arpan Pal. 2016. Shake meter: An Autonomous Vibration Measurement System using Optical Strobing: Demo Abstract. In *Proceedings of the 14th ACM Conference on Embedded Network Sensor Systems CD-ROM.* ACM, 294–295.

[10] Simon J Sheather and Michael C Jones. 1991. A reliable data-based bandwidth selection method for kernel density estimation. *Journal of the Royal Statistical Society. Series B (Methodological)* (1991), 683–690.

[11] Ashok Veeraraghavan, Dikpal Reddy, and Ramesh Raskar. 2011. Coded strobing photography: Compressive sensing of high speed periodic videos. *IEEE Transactions on Pattern Analysis and Machine Intelligence* 33, 4 (2011), 671–686.

[12] X-G Xia. 2000. An efficient frequency-determination algorithm from multiple undersampled waveforms. *IEEE Signal Processing Letters* 7, 2 (2000), 34–37.

[13] Xiang-Gen Xia and Kejing Liu. 2005. A generalized Chinese remainder theorem for residue sets with errors and its application in frequency determination from multiple sensors with low sampling rates. *IEEE Signal Processing Letters* 12, 11 (2005), 768–771.

[14] Hanshen Xiao and Guoqiang Xiao. 2017. Notes on CRT-based robust frequency estimation. *Signal Processing* 133 (2017), 13–17.

[15] Li Xiao and Xiang-Gen Xia. 2014. A generalized Chinese remainder theorem for two integers. *IEEE Signal Processing Letters* 21, 1 (2014), 55–59.